arXiv:cond-mat/0501573v1 [cond-mat.soft] 24 Jan 2005

Effective pair interactions between colloidal particles at a nematic-isotropic interface

D. Andrienko[1], M. Tasinkevych[2,3] and S. Dietrich[2,3]

[1] *Max-Planck-Institut für Polymerforschung - Ackermannweg 10, 55128 Mainz, Germany*

[2] *Max-Planck-Institut für Metallforschung - Heisenbergstr. 3, 70569 Stuttgart, Germany*

[3] *Institut für Theoretische und Angewandte Physik, Universität Stuttgart - Pfaffenwaldring 57, 70569 Stuttgart, Germany*

PACS. 61.30.Dk – Continuum models and theories of liquid crystal structure.
PACS. 82.70.Dd – Colloids.
PACS. 61.30.Jf – Defects in liquid crystals.

Abstract. – The Landau-de Gennes free energy is used to study theoretically the interaction of parallel cylindrical colloidal particles trapped at a nematic-isotropic interface. We find that the effective interaction potential is non-monotonic. The corresponding force-distance curves exhibit jumps and hysteresis upon approach/separation due to the creation/annihilation of topological defects. Minimization results suggest a simple empirical pair potential for the effective colloid-colloid interaction at the interface. We propose that the interface-mediated interaction can play an important role in self-organization and clustering of colloidal particles at such interfaces.

Introduction. – Colloidal particles dissolved in a nematic solvent experience long-ranged interactions [1]. These effective interactions are generated by the distortions of the liquid crystal director around the particles and result in their clustering and self-organization [2, 3]. Upon approaching and at the nematic-isotropic transition, the solvent forms nematic and isotropic domains, which leads to an additional interaction of the particles with the interface between the two phases [4, 5]. The resultant morphology of the network formed by the particles in colloid-liquid crystal composites is very sensitive to this interaction [4, 6]. In fact, colloidal particles can be captured by the nematic-isotropic interface and even dragged by a *moving* interface [4]. This enables one to manipulate tiny particles in suspension, which in a more general context is of technological importance for manufacturing of *e*-papers and electrophoretic displays [7], separation of bacterial species and living cells [8], trapping of DNA and polymer particles [9], as well as growth of photonic crystals [10]. The structures of self-assembled colloid layers at *free* surfaces of nematic films can be tuned by their thickness [11].

Recent experiments of dragging colloidal particles by nematic-isotropic interfaces [4] demonstrated that a single colloidal particle is attracted by the interface. This conclusion is in accordance with theoretical results obtained by minimizing the corresponding Landau-de Gennes

© EDP Sciences

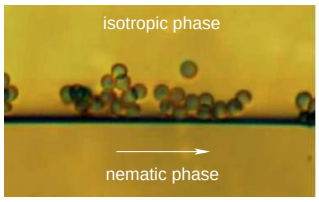


Fig. 1

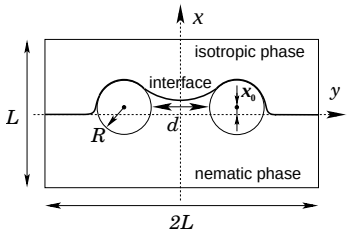


Fig. 2

Fig. 1 – Aggregates of 16 μm polymer particles captured by a nematic-isotropic interface. The director is parallel to the nematic-isotropic interface and lies within the plane of the figure. In the experiment the interface moves in the upward direction and drags the colloids. Courtesy of A. Glushchenko, J. L. West, G. Liao, and Yu. Reznikov, Liquid Crystal Institute, Kent, Ohio, USA.

Fig. 2 – Cross-section of two parallel cylindrical particles trapped at a nematic-isotropic interface at $x = 0$. The system is translationally invariant in z-direction.

free energy [5]. The resulting force on the particle is non-monotonic and is roughly proportional to the particle radius. Experimental results [4] also suggested that the particles captured by the interface interact with each other differently than in the pure nematic or isotropic phase, e.g., the particle-particle interaction depends on the interfacial curvature; particles which interact only weakly in the bulk can segregate and form two-dimensional clusters once they are captured by the interface (see Fig. 1).

The appearance of additional interface induced features in the interaction between colloidal particles can be expected from analogous phenomena at interfaces of simple fluids [12] which, however, still pose unresolved challenges in understanding [13]. In liquid crystals the situation is even more complicated. The director deformations extend into the nematic phase, i. e., in addition to interfacial energies, the bulk elasticity contributes to the total free energy of the system. The effective surface tension (provided it can be introduced in the first place) depends on the orientation of the director, which in turn varies along the interface. The boundary conditions for the director at the particle surfaces give rise to topological defects accompanying the particles. In order to minimize the free energy associated with the director distortions as well as the free energy of the defect cores, the defects often merge with the isotropic phase [5] or with each other.

The combination of the above-mentioned effects enriches the phenomena significantly but complicates their theoretical understanding enormously: expressions for the director field, the free energy, or force-distance profiles can hardly be obtained analytically. Numerical calculations are also not straightforward because the interfacial width and the size of the defect cores are normally much smaller that the size of the colloidal particle, so that there are several rather different length-scales involved. Therefore significant computational efforts involving finite-element methods with adaptive meshes are required to address even static problems [14].

In the following we study the interaction of two long parallel cylindrical colloids trapped at a (initially) flat nematic-isotropic interface. We find that their effective interaction is rather complex: the force-distance profiles can exhibit jumps and hysteresis upon approach or separation. The particles can either repel or attract each other depending on the material parameters and the geometry. Finally, we propose a simple effective pair potential which can be exploited to study clustering and self-organization of colloids at NI interfaces.

Landau–de Gennes free energy. – Two identical colloidal particles, each of which we take to be a long cylinder of radius R with the symmetry axis parallel to the z axis, are immersed into a nematic liquid crystal at a separation d, see Fig. 2. The nematic order parameter tensor at the boundaries is fixed in a such a way that without the colloids a flat nematic-isotropic interface is formed at $x = 0$. The order parameter at the top wall is fixed to zero; the absolute value of the order parameter at the bottom wall is fixed to the bulk order parameter of the nematic phase at two-phase coexistence. The director orientation at the bottom wall is also fixed and corresponds to the preferred director anchoring at the nematic-isotropic interface, i.e., parallel or perpendicular to the interface. The axes of the particles are positioned at $x = x_0$. In the course of the free energy minimization x_0 adjusts itself such that that the $x-$component of the force exerted on the particles vanishes.

The system is characterized by the Landau-de Gennes free energy [15]

$$F = \int dV \Big[a(T-T^*)Q_{ij}Q_{ji} - bQ_{ij}Q_{jk}Q_{ki} + c(Q_{ij}Q_{ji})^2 + \frac{L_1}{2}Q_{ij,k}Q_{ij,k} + \frac{L_2}{2}Q_{ij,j}Q_{ik,k} \Big], \quad (1)$$

where summation over repeated indices is implied and the comma indicates the spatial derivative. The positive constants a, b, c are assumed to be temperature independent, and T^* is the supercooling temperature of the isotropic phase. The constants L_1 and L_2 are related to the Frank-Oseen elastic constants $K_{11} = K_{33} = 9Q_b^2(L_1 + L_2/2)/2$ and $K_{22} = 9Q_b^2 L_1/2$ and Q_b is the bulk nematic order parameter. The sign of L_2 determines the preferred orientation of the director at the nematic-isotropic interface. $L_2 > 0$ ($L_2 < 0$) favors planar (perpendicular) anchoring. We introduce the dimensionless temperature $\tau = 24ca(T - T^*)/b^2$. The bulk nematic phase is stable for $\tau < \tau_{\rm NI} = 1$ with a degree of orientational order given by $Q_b = b(1 + \sqrt{1 - 8\tau/9})/8c$; $Q_b(\tau > 1) = 0$.

We consider both rigid homeotropic and finite anchoring boundary conditions at the colloidal surfaces. In the latter case the surface free energy density is taken as [16] $f_s = \frac{1}{2}w{\rm Tr}(\boldsymbol{Q} - \boldsymbol{S})^2$ where w is the anchoring coefficient and $S_{\alpha\beta} = S\left(e_\alpha e_\beta - \delta_{\alpha\beta}/3\right)$ is the preferred tensor order parameter at the colloid surface with $\boldsymbol{e}$ as the unit vector along the easy axis direction.

For the constants entering the free energy density (Eq. (1)) we use typical values for a nematic compound 5CB [17]: $a = 0.044\times10^6\,{\rm J/m^3K}$, $b = 0.816\times10^6\,{\rm J/m^3}$, $c = 0.45\times10^6\,{\rm J/m^3}$, $L_1 = 6\times10^{-12}\,{\rm J/m}$, $T^* = 307\,{\rm K}$. The choices for L_2 will be given below. The nematic-isotropic transition temperature for 5CB is $T_{NI} = 308.5\,{\rm K}$. At coexistence the nematic coherence length (i.e., the thickness of the nematic-isotropic interface) is $\xi = \left(24L_1c/b^2\right)^{1/2} \approx 10\,{\rm nm}$ which sets the smallest length-scale of our description.

The equilibrium distribution of the tensor order parameter Q_{ij} is obtained by minimizing the free energy functional (1) numerically using finite elements with adaptive meshing. The area $L\times2L$ is triangulated and the functions Q_{ij} are linearly interpolated within each triangle.

Planar interfacial anchoring. – For this case we chose the anisotropy of the elastic constants as $L_2/L_1 = 2$, favoring director alignment parallel to the NI interface and in the plane $z = 0$. We use rigid homeotropic boundary conditions at the colloidal surfaces. Upon minimizing the free energy we have identified two stable orientational configurations. At sufficiently large separations d both colloids are accompanied by a defect of strength 1/2 (Fig. 3(b)). If the particles move closer, the two defects merge and form a single, but rather extended, defect positioned between the colloids (Fig. 3(a)). We have also observed three metastable configurations. Here either one of the defects, Fig. 3(c), or even both defects, Fig. 3(d) and (e), merge with the isotropic phase: the system is trying to reduce its free energy by annihilating the defects. However, the interface has to bend and almost wrap

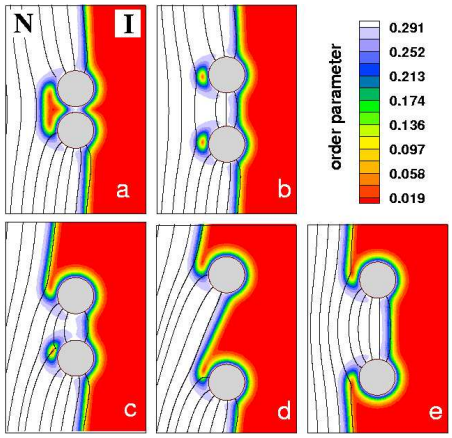


Fig. 3

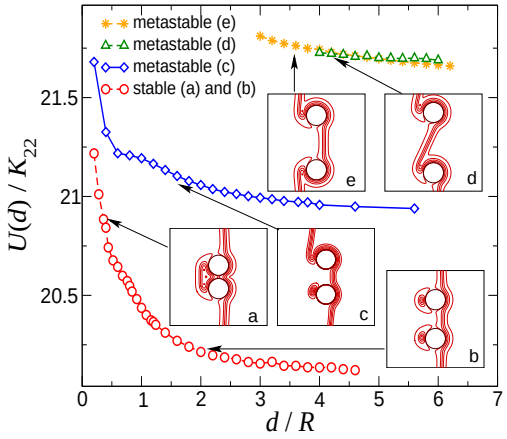


Fig. 4

Fig. 3 – Order parameter and director maps for stable {a,b} and metastable {c,d,e} configurations. Particle radius $R/\xi = 5$; elastic constants favor planar anchoring at the nematic-isotropic interface. Solid lines indicate the local director orientation. There is translational symmetry along the z axis and the director lies in the xy plane.

Fig. 4 – Effective pair potential $U(d)$ per unit length for planar director anchoring at the NI interface and homeotropic anchoring at the colloid surface, for both stable and metastable configurations with $R/\xi = 5$. The insets depict the corresponding configurations by iso-order-parameter lines.

the particles in order to reach the defects. This of course increases the interfacial energy, which is roughly proportional to the area of the interface. For small separations, among the metastable configurations only the one shown in Fig. 3(c) is possible: due to strong anchoring at the particle surfaces the nematic phase forms a bridge between the particles, preventing the isotropic phase from reaching also the second defect. For larger separations, the isotropic phase can extend partially around the colloids and merge with the second defect. This can occur asymmetrically, as shown in Fig. 3(d), or symmetrically, see Fig. 3(e).

The effective pair potential $U(d)$ defined as the free energy per length of the colloidal particles is presented in Fig. 4. In all cases the particles repel each other. The branch of $U(d)$ which corresponds to the *stable* configurations, reveals practically no breaks in slope, even though at $d/R \approx 0.4$ the director field around the particles changes abruptly between the configurations (a) and (b). However, if one of the metastable configurations is present in the system, transitions between different branches can occur giving rise to jumps and hysteresis in the force-distance curves upon particle approach/separation.

Homeotropic anchoring at the interface. – The choice $L_2/L_1 = -1/2$ for the anisotropy of the elastic constants favors director alignment perpendicular to the NI interface in the plane $z = 0$. In this case we have found only two, stable configurations. The first one, containing a defect, is shown in Fig. 5(a). It occurs at small separations, where the nematic bridge between the particles forces the director to be parallel to the interface. The other configuration has no defects, because the nematic bridge with director orientation parallel to the interface disappears and the defect merges with the isotropic phase.

The corresponding effective potential $U(d)$ is shown in Fig. 6. As in the previous case, the particles repel each other at small separations where there are large director distortions in the inter-particle region. However, contrary to the case with planar anchoring, there is a

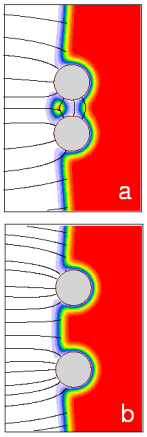


Fig. 5

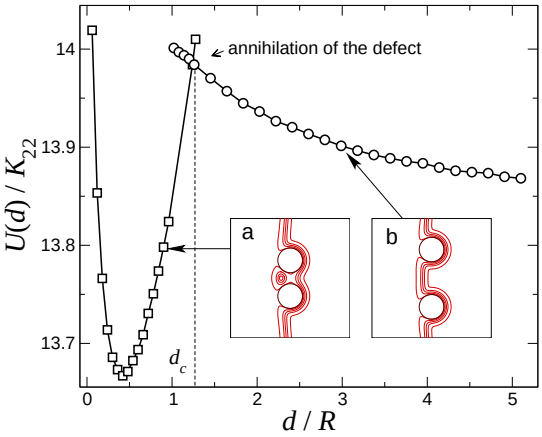


Fig. 6

Fig. 5 – Director and order parameter maps for homeotropic anchoring at the NI interface corresponding to elastic constants $L_2 = -1/2L_1$ and particle radius $R/\xi = 5$. Configuration (a) is stable at short distances, (b) at large distances.

Fig. 6 – Effective pair potential $U(d)$ per unit length for homeotropic anchoring at the NI interface, $L_2 = -1/2L_1$, homeotropic anchoring at the colloid surface, and $R/\xi = 5$. The configuration with the defect results in strong attraction at short distances. There is repulsion at large distances. The insets characterize the corresponding configurations by iso-order-parameter lines (see Fig. 5). For $d < d_c$ configuration (b) is metastable.

strong attraction between the particles for $d/R \lesssim 1$, where the configuration with the defect is stable. The branch without the defect results in weak repulsion, as for planar anchoring.

Empirical expression for the effective potential. – Minimization of the free energy is a computationally expensive task, which cannot be used, for example, to calculate the forces on the particles each time their positions are advanced using molecular dynamics or Monte-Carlo algorithms for their kinetics. Use of effective potentials is a typical solution to this problem.

In order to find such an appropriate potential we have calculated the free energy per unit length for particles of different radii, $R/\xi \approx 2.5-12.5$, corresponding to $R \approx 0.025-0.125\,\mu$m. Since colloids are rather small, the finite director anchoring at the particle surfaces has to be taken into account. We have used a value appropriate for 5CB on a polymer surface [18], $w\xi/L_1 = 0.822$; for this energy the dimensionless anchoring parameter $\eta = wQ_b^2 R/K_{22}$ is of the order of 1.

Minimization results for both planar and homeotropic anchoring of the director at the interface are shown in Fig. 7 (a) and (b). The strong repulsion close to contact ($d = 0$) has become smoother for planar and disappeared for homeotropic anchoring at the interface, due to the finite director anchoring at the colloid surfaces. It turns out that in both cases the following shape of the potential fits the numerical data very well:

$$U(d) = \begin{cases} U_a\left[1+\gamma(d/\xi)^2\right], & 0 \le d \le d_c \\ U(\infty) + U_0\Big(\exp\left[-\alpha\,(d/\xi)^{-\beta}\right] - 1\Big), & d > d_c, \end{cases} \tag{2}$$

where α, β, γ are (positive) fitting parameters. The first part of the potential ($0 \le d \le d_c$) describes a simple harmonic-type attraction between the particles, which we observed for the

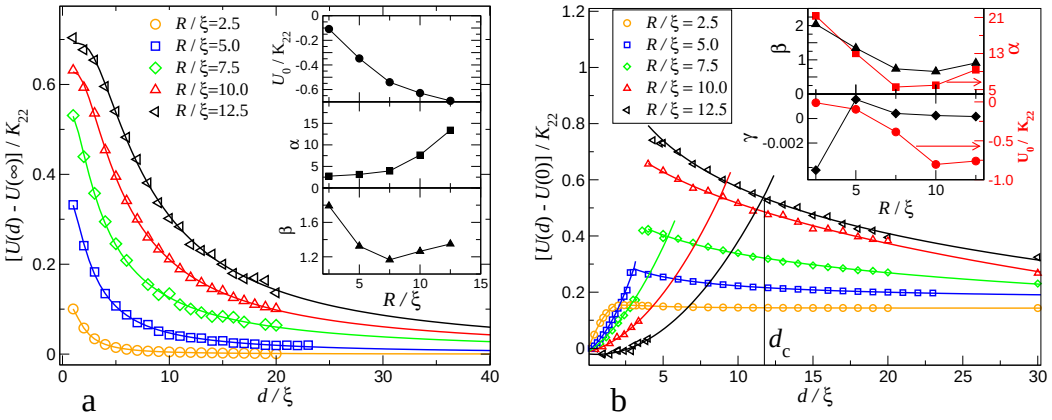


Fig. 7 – Effective pair potential as a function of the distance d between colloids for different colloid radii R: (a) planar and (b) homeotropic anchoring of the director at the interface and finite anchoring at the colloid surface. Symbols: minimization results; solid lines: fit to the empirical equation (2). Inset illustrates the dependence of the fitting parameters on R. $\xi = 10\,\mathrm{nm}$, $K_{22} = 2.6 \times 10^{-12}\,\mathrm{J/m}$. $U_a/K_{22} \approx 6.8 - 26.5$ corresponding to $R/\xi \approx 2.5 - 12.5$.

homeotropic anchoring; for *planar* interfacial anchoring $d_c \equiv 0$. In the case of homeotropic anchoring d_c is a critical distance at which the defect annihilates (see Figs. 5 and 6).

We have no analytical support for the functional form of the effective potential (2). However, qualitatively, the effective interaction of the colloidal particles in a bulk nematic phase is known to exhibit a power-law decay at large distances [1]. In our case, the leading term of the expansion for $d/\xi \to \infty$ is indeed $\sim (d/\xi)^{-\beta}$. On the other hand, if two colloids are sufficientlly close, so that the regions where the *order parameter* changes from their surface to the bulk value start to overlap, and where the defects (if present) interact with each other and the particles [14], the functional form of the potential changes. Normally, the distortions of the order parameter relax exponentially (similar to the variations of the order parameter through the nematic-isotropic interface) resulting in an exponentially varying strength of the interaction. This is also captured qualitatively by the potential given in Eq. (2).

The fitting curves are also shown in Fig. 7 (a) and (b). For planar anchoring $\beta \approx 1.5$; for homeotropic anchoring $\beta \approx 1.0$, i. e., in both cases the interaction potential is long-ranged. In case of homeotropic anchoring there is a critical size of colloidal particles (of the order of interfacial width) below which the discontinuous structural transition between the configurations with and without the defect disappears. Similar phenomena, named capillary bridging, can be observed in granular materials, liquid crystals, and binary mixtures [19]. In all cases, one of the phases (otherwise metastable in the bulk) condenses out and forms a bridge between the particles. This transition is discontinuous and ends in a critical point for small particle radii. In our case, the nematic phase located between the isotropic phase and the defect forms a bridge between the particles and results in their attraction.

Conclusions. – In conclusion, within the Landau-de Gennes formalism we have studied the effective pair interaction between two cylindrical parallel colloids trapped at the nematic-isotropic interface. This pairwise interparticle force depends sensitively on the radii of colloids, the orientation of the director at the NI interface, and the anchoring strength, i.e., the nematic elasticity is an essential ingredient of the interaction. The formation or annihilation of defects influences the effective pair potential. It also changes the repulsive character of the interaction

at large separations to an attractive one at intermediate or small separations. Therefore, one should expect that many-body interactions are relevant to describe collective colloidal ordering at the interface. Another implication of our work is that the interface is able to rearrange the nucleation centers of, for example, phase-separating polymer network and help to design composite materials of extraordinary properties.

* * *

We thank to M. Deserno, A. Glushchenko, K. Kremer, G. Liao, M. Oettel, Yu. Reznikov, and J. L. West for useful discussions.

REFERENCES

[1] S. Ramaswamy, R. Nityananda, V. Raghunathan and J. Prost, *Mol. Cryst. Liq. Cryst*, **288** (1996) 175; T. C. Lubensky, D. Pettey, N. Currier and H. Stark, *Phys. Rev. E*, **57** (1998) 610; H. Stark, *Eur. Phys. J. B*, **10** (1999) 311.
[2] J. C. Loudet and P. Poulin, *Phys. Rev. Lett.*, **87** (2001) 165503; V. J. Anderson, E. M. Terentjev, S. P. Meeker, J. Crain and W. C. K. Poon, *Eur. Phys. J.*, **4** (2001) 11.
[3] P. Poulin, H. Stark, T. C. Lubensky and D. A. Weitz, *Science*, **275** (1997) 1770.
[4] J. L. West, A. Glushchenko, G. X. Liao, Y. Reznikov, D. Andrienko and M. P. Allen, *Phys. Rev. E*, **66** (2002) 012702.
[5] D. Andrienko, M. Tasinkevych, P. Patricio and M. M. T. da Gama, *Phys. Rev. E*, **69** (2004) 021706.
[6] D. Vollmer, G. Hinze, W. C. K. Poon, J. Cleaver and M. E. Cates, *J. Phys.: Condens. Matter*, **16** (2004) L227.
[7] R. Zehner, K. Amundson, A. Knaian, B. Zion and M. Johnson, *SID 03 Digest*, (2003) 842.
[8] H. A. Pohl, *Dielectrophoresis* (Cambridge University Press, Cambridge) 1978; G. H. Markx, P. A. Dyda and R. Pethig, *J. Biotechnol.*, **51** (1996) 175.
[9] M. Washizu, *J. Electrost.*, **25** (1990) 109; H. Morgan, M. P. Hughes and N. G. Green, *Biophys. J.*, **77** (1999) 516.
[10] K. Yoshinaga, M. Chiyoda, A. Yoneda, H. Nishida and M. Komatsu, *Colloid Polym. Sci.*, **277** (1999) 479.
[11] I. I. Smalyukh, S. Chernyshuk, B. I. Lev, A. B. Nych, U. Ognysta, V. G. Nazarenko and O. D. Lavrentovich, *Phys. Rev. Lett.*, **93** (2004) 117801.
[12] P. A. Kralchevsky and K. Nagayama, *Adv. Colloid Interface Sci.*, **85** (2000) 145; M. G. Nikolaides, A. R. Bausch, M. F. Hsu, A. D. Dinsmore, M. P. Brenner, C. Gay and D. A. Weitz, *Nature*, **420** (2002) 299;
[13] L. Foret and A. Würger, *Phys. Rev. Lett*, **92** (2004) 058302; M. Oettel, A. Domínguez, and S. Dietrich, *preprint,* cond-mat/0411329, (2004) .
[14] M. Tasinkevych, N. M. Silvestre, P. Patrício and M. M. Telo da Gama, *Eur. Phys. J. E*, **9** (2002) 341; P. Patrício, M. Tasinkevych and M. M. Telo da Gama, *Eur. Phys. J. E*, **7** (2002) 117.
[15] P. G. de Gennes and J. Prost, *The Physics of Liquid Crystals* (Clarendon Press, Oxford) 1995.
[16] M. Nobili and G. Durand, *Phys. Rev. A*, **46** (1992) R6174.
[17] S. Kralj, S. Žumer and D. W. Allender, *Phys. Rev. A*, **43** (1991) 2943.
[18] D. Andrienko, Y. Kurioz, M. Nishikawa, Y. Resnikov and J. L. West, *Jpn. J. Appl. Phys.*, **39** (2000) 1217.
[19] H. Stark, J. Fukuda, and H. Yokoyama, *Phys. Rev. Lett.*, **92** (2004) 205502; D. Andrienko, P. Patrício and O. I. Vinogradova, *J. Chem. Phys.*, **121** (2004) 4414; T. C. Halsey and A.

J. Levine, *Phys. Rev. Lett.*, **80** (1998) 3141; C. Bauer, T. Bieker, and S. Dietrich, *Phys. Rev. E*, **62** (2000) 5324.